Journal of Hydraulic Structures
J. Hydraul. Struct., 2021; 7(1):1-15
DOI: 10.22055/jhs.2021.36839.1164

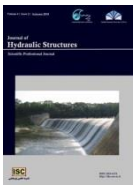

OPEN ACCESS

Turbulent Flow Modeling at Tunnel Spillway Concave Bends and Prediction of Pressure using Artificial Neural Network

Zeinab Bashari Moghaddam [1]
Hossein Mohammad Vali Samani[2]
Seyed Habib Mousavi Jahromi [3]

Abstract

A tunnel spillway is one of the spillway types in which a high free surface flow velocity is established. The pressure increases in concave vertical bends due to the rotational acceleration and the nature of irregularities in the turbulent flow. Physical models are the best tools to analyze this phenomenon. The number of the required physical models to cover all practical prototype condition analysis is so large that makes it impractical in terms of placement and costs. Therefore, the FLOW-3D software has been chosen to analyze and produce a database of turbulent flow in tunnels concave bends covering all possible practical alternatives. Various tunnels with different discharges and geometries have been simulated by this software. The numerical results were verified with the experimental ones of the constructed physical model of Alborz Dam tunnel spillway, and a satisfactory agreement was obtained. Dimensional analysis is used to group the involved variables of the problem into dimensionless parameters. These parameters are utilized in the artificial neural network simulation. The results showed a correlation coefficient R2=0.95 between the dimensionless parameters obtained by the Flow-3D software and those predicted by the neural network which leads to the conclusion that the artificial neural network based on the database obtained by the turbulent flow modeling in this regard is a powerful tool for pressure prediction.

Keywords: Flow-3D, Tunnel spillway concave bend, Numerical simulation, Turbulent flow, Artificial neural network

Received: 04 March 2021; Accepted: 11 April 2021

[1] Department of Civil Engineering, Shahr-e-Qods Branch, Islamic Azad University, Tehran, Iran. ORC-ID: 0000-0001-6145-9104
[2] Department of Civil Engineering, Shahr-e-Qods Branch, Islamic Azad University, Tehran, Iran. E-Mail: E-mail: hossein.samani@gmail.com ORC-ID: 0000-0003-3645-2271 **(Corresponding Author)**
[3] Department of Civil Engineering, Shahr-e-Qods Branch, Islamic Azad University, Tehran, Iran. ORC-ID: 0000-0002-9450-460x

1. Introduction

Spillways are designed to release floods through reservoirs downstream of the dams. A tunnel spillway is one of the common types used in dam construction which consists of an inlet, along with a vertical or inclined shaft and a horizontal tunnel. The shaft is connected to the horizontal channel by a concave bend with a curvature radius proportional to the tunnel diameter. The concave curvature results in additional pressure due to the rotational movement of the flow in this area. The phenomenon is so complicated that makes the development of an explicit accurate relationship very difficult.

Many three-dimensional numerical studies have been done on spillways to obtain flow depth profiles, velocity, and pressure distributions (Kim and Park, [1]; Sabbagh-Yazdi et al., [2]; Nohani, [3]; Parsaie et al., [4]; Teuber et al., [5]; Ghazanfari-Hashemi et al., [6]).

Numerical turbulent flow simulations have led to great successes in operational programs for spillways on large scales (Sha et al., [7]; Liu et al., [8]; Zheng et al.,[9]; Hongmin et al., [10]; Wan et al., [11]; Wei et al., [12]). Comparison of numerical and experimental results performed by many researchers showed good agreements (Xu et al., [3]; Huang et al., [14]; Li et al., [15]; Shilpakar et al., [16]). Song and Zhou [17], proposed a three-dimensional model of a tunnel-shaped spillway's flow. They applied the large eddy simulation (LES) to determine the effects of turbulence and the freeflow surface was determined based on the Eulerian-Lagrangian approach. The steady spillway flow was solved by the Bernoulli formula. Subsequently, the problem was analyzed in three dimensions based on the governing equations considering the fixed free surface flow. Finally, the entire field was calculated based on a variable free flow surface. In comparison to the experimental results, the numerical results showed high accuracy. Fais et al. [18] studied the hydraulic behavior of this type of knee joint compared to the 90-degree knee joint and multi-center knee joint. The results showed that the parabolic knee joint made by them increases the discharge capacity of the morning glory spillway.

Pressure relationships in the bends of tunnel spillways obtained by former studies are few. The most common relationships are given below. Falvey [19], suggested the following relationship to calculate the flow pressure distribution in the concave curvature:

$$P = \gamma \left[h\cos\theta + \left(1 - \frac{h}{2R}\right)\left(\frac{h}{R}\right)\frac{V}{g}\right] \quad (1)$$

In which P is the total pressure at the bed of the curvature, V is the mean flow velocity which is equal to the flow discharge divided by the flow cross-sectional area, R is the radius of curvature, h is the flow depth, ρ is the fluid density, g is the gravitational constant, γ is the unit weight of the fluid, θ is the slope angle of the tunnel bed, and D is the tunnel diameter.

To determine the pressure distribution of the flow in concave curvatures such as those of the tunnel spillways, the forces acting vertically in a fluid column should be considered (see Fig. (1)). The pressure at the end of the fluid column is caused by its weight and the force resulting from centrifugal acceleration. The total pressure given by Chaudhry, [20], is

$$P = \gamma h\left(1 + \frac{V^2}{gR}\right) \quad (2)$$

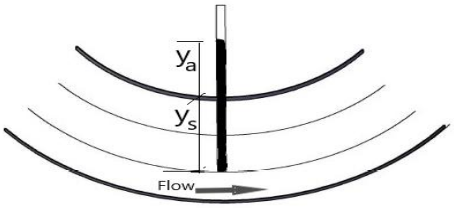

Figure 1. Flow in a concave curvature

In which y_s is static pressure head and y_a is head due to rotational flow acceleration.

Most of the studies on bends in hydraulic structures have focused on the curvature of flip buckets. Involved flip bucket flow variables are depicted in Fig. (2). Novak et al. [21], developed the following relationship for the pressure distribution on the bed of the flip bucket:

$$P = \gamma h \cos\theta + \rho V^2 \ln\left(\frac{R}{R-h}\right) \quad (3)$$

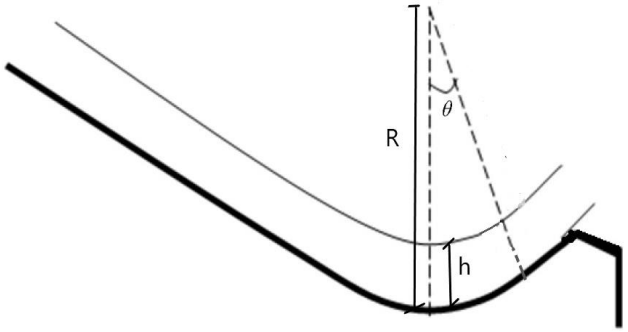

Figure 2. Flow in the curvature of the flip bucket

Jorabloo et al. [22], obtained the velocity distribution at the curvature of the flip bucket, using the standard k-ε turbulent flow model, which revealed a good accord with experimental results. Khani et al. [23], used the FLOW-3D software and RNG turbulent flow model to calculate the pressure distribution in the curvature of flip buckets used various discharges and made a comparison with experimental results. They found that maximum pressures occur close to the middle of the curvatures. Besides, unlike theoretical relationships, numerical turbulent simulations produce remarkable pressure and velocity oscillations.

An artificial neural network (ANN) is a computational or mathematical model that is inspired by the structure or functional aspects of biological neural networks. When the relationship between data is unknown, ANN proves to be a powerful tool. ANN can easily identify and learn interconnected patterns between input data sets and corresponding target values.

The development of ANN performs a nonlinear mapping between inputs and outputs. ANN was first developed in the 1940s (McCulloch and Pitts,[24]), and the development has experienced a revival with Hopfield's effort (Hopfield, [25]). Wu et al. [26] contrasted the simulation results of the discharge coefficient function method, the average value method, and the artificial neural network method, analyzing the applicability of these three methods. The

most widely used method for discharge coefficient simulation is regression analysis (Qiu et al, [27]; Xiang et al, [28]; Ye and He,[29]), which not only achieves higher precision but also solves some practical problems. Salmasi et al. [30] used the Genetic Programming (GP) algorithm and ANN techniques to forecast the discharge coefficient of the wide crest weir, obtaining two regression equations. Through the analysis of the equation simulation effect, it was found that the GP algorithm is more efficient than ANN, with sufficiently accurate measurement results. ANN was employed by Noori and Hoshiarpur [31] based on the major effects of the input parameters on the downstream scouring of the fillip bucket. Their results showed that the Log–Sigmaid model had a good performance in the modeling of the depth of scouring. The smooth particle hydrodynamics technique was adopted to study pressure distribution on the steps of a stepped spillway.

In this research the neaural network based on a database obtained by the Flow-3D turbulent flow model is used to fit the data and predict the pressure distribution at the concave bends of the tunnel spillways.

2. Materials and methods

In the present study, various dimensions of tunnel spillways and different discharges which cover almost all practical cases are used in the simulation by the FLOW-3D program. The involved variables are combined to produce dimensionless groups using dimensional analysis. The results of the numerical modeling are used in these dimensionless groups to produce a database in which the pressure at the concave bends of the tunnel spillways is a function of other variables involved in the dimensionless parameters. The relationship between these dimensionless parameters is unknown. Hence, the best tool of data fitting for such a problem is the ANN technique by which the pressure distribution at concave bends of tunnel spillways can be predicted.

In this research, the FLOW-3D (Ver. 11.0.4) was used to simulate the flow field in tunnel spillways. FLOW-3D is an accurate, fast, proven CFD software that solves the toughest free-surface flow problems. A pioneer in the CFD industry, and a trusted leader, FLOW-3D is a highly-efficient, comprehensive solution for turbulent free-surface flow problems. Various turbulent flow models such as the $k-\varepsilon, k-\omega$, and RNG can be employed in this software. Flow-3D software is chosen because it is very easy to use and reliable. Besides, it has the advantages of being able to be linked to the AutoCAD program.

Various tunnel diameters, curvatures, and discharges that cover all practical cases were used in the simulations. The results were verified with the experimental ones obtained from the physical model of Alborz Dam spillway and it was found that the RNG method is the best for 3D turbulent flow modeling in tunnel spillways.

The governing equations of the time-averaged turbulent flow (continuity and Navier-Stokes's equations) which are solved in turbulent modeling are given below:

$$\frac{\partial\,\bar{u}}{\partial x}+\frac{\partial\,\bar{v}}{\partial y}+\frac{\partial\,\bar{w}}{\partial z}=0 \tag{4}$$

$$\frac{\partial\,\bar{u}}{\partial\,t}+\bar{u}\,\frac{\partial\,\bar{u}}{\partial x}+\bar{v}\frac{\partial\,\bar{u}}{\partial y}+\bar{w}\frac{\partial\,\bar{u}}{\partial z}=g_x-\frac{1}{\rho}\frac{\partial\,\bar{P}}{\partial x}+\nu_t\nabla^2\bar{u}-\underbrace{\left(\frac{\partial\,\overline{\acute{u}\acute{u}}}{\partial x}+\frac{\partial\overline{\acute{u}\acute{v}}}{\partial y}+\frac{\partial\overline{\acute{u}\acute{w}}}{\partial z}\right)}_{1} \tag{5}$$

$$\frac{\partial\,\bar{v}}{\partial\,t}+\bar{u}\,\frac{\partial\,\bar{v}}{\partial x}+\bar{v}\frac{\partial\,\bar{v}}{\partial y}+\bar{w}\frac{\partial\,\bar{v}}{\partial z}=g_y-\frac{1}{\rho}\frac{\partial\,\bar{P}}{\partial y}+\nu_t\nabla^2\bar{v}-\underbrace{\left(\frac{\partial\,\overline{\acute{u}\acute{v}}}{\partial x}+\frac{\partial\overline{\acute{v}\acute{v}}}{\partial y}+\frac{\partial\overline{\acute{v}\acute{w}}}{\partial z}\right)}_{2} \tag{6}$$

$$\frac{\partial\ \bar{w}}{\partial\ t}+\ \bar{u}\ \frac{\partial\ \bar{w}}{\partial x}+\bar{v}\frac{\partial\ \bar{w}}{\partial y}+\bar{w}\frac{\partial\ \bar{w}}{\partial z}=g_z-\frac{1}{\rho}\frac{\partial\ \bar{p}}{\partial z}+\ \nu_t\nabla^2\bar{w}-(\underbrace{\frac{\partial\ \overline{\acute{u}\acute{w}}}{\partial x}+\frac{\partial\overline{\acute{v}\acute{w}}}{\partial y}+\frac{\partial\overline{\acute{w}\ \acute{w}}}{\partial z}}_{3}) \quad (7)$$

In the above equations, ($\bar{u}$,$\bar{v}$,$\bar{w}$) are the velocity components averaged by time in three directions of coordinates, x, y, and z. $g_x, g_y,$ and g_z are the components of the gravity acceleration in x, y, and z directions. ν_t is the turbulent viscosity, and the terms 1, 2, and 3 in the time-averaged Navier-Stokes's equations are the Reynolds stresses. The variety of turbulent flow models is in the turbulent viscosity modeling. These models include zero-equation models, one-equation models, two-equation models, models with stress equations, and large eddy simulation models. In the present research, the RNG model was chosen since it gave the best agreement with the real results of the physical model of the tunnel spillway of Alborz Dam. The RNG model is similar to the standard k-ε model. The only difference between the two models is that in the RNG model, the equation has been modified so that it can consider various movement scales [32]. This method was innovated by Yakhot et al. [33] Governing equations in this method include:

$$\frac{\partial k}{\partial t}+\bar{u}_i\frac{\partial k}{\partial x_i}=\nu_t\ S^2-\varepsilon\ +\frac{\partial}{\partial x_i}\left(\alpha\,\nu_t\frac{\partial k}{\partial x_i}\right) \quad (8)$$

$$\frac{\partial \varepsilon}{\partial t}+\bar{u}_i\frac{\partial \varepsilon}{\partial x_i}=C_{\epsilon 1}\frac{\varepsilon}{k}\ \nu_t\ S^2-C_{\epsilon 2}\frac{\varepsilon^2}{k}-\bar{R}+\frac{\partial}{\partial x_i}\left(\alpha\,\nu_t\frac{\partial \varepsilon}{\partial x_i}\right) \quad (9)$$

In which $\eta=\frac{Sk}{\varepsilon}$, and S shows the strain. $C_{\epsilon 1}$, $C_{\epsilon 2}$, C_μ, η_0, and β are constant coefficients. In this method, k and ε are calculated through the solution of Eqs. (8) and (9). Then, using the relationships $\nu_{eddy}=C_\mu\frac{k^2}{\varepsilon}$ and $\nu_t=(\nu_{eddy}-\nu_o)$, the turbulent viscosity is determined and used to solve the Reynolds averaged Navier-Stokes's equations.

2.1. Verification of the numerical results

In this research, 117 tunnels with the range of diameters from 3 to 15 m, three different radii of curvatures, equal to two, three, and four times the diameter, and three discharges from low to high were simulated. Given the complex geometry of the tunnel spillway, the initial geometry of the model was plotted in AutoCad3D and given to the FLOW-3D software. To verify the numerical results, the experimental results of the physical model of the tunnel spillway of Alborz storage dam, provided by the water research center of the ministry of energy in Iran [34], were used. In this model, three discharges of 600, 800, and 950 m^3/s were considered. Table 1 lists the results of the pressure heads for various discharges obtained by the numerical model and experiments in seven points at the bed of the concave curvature (Fig. (3)). The tunnel diameter is 7.5 m and the radius of the concave curvature is 18.75 m.

The mean absolute relative error which shows the difference between the numerical and experimental results is calculated according to:

$$MARE = \frac{\sum \frac{|H_e - H_n|}{H_e}}{N} \times 100 \quad (11)$$

In which H_n is Numerical pressure head, H_e is Experimental heads, and N is the number of data.

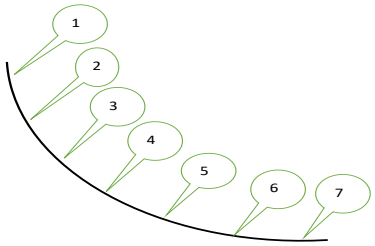

Figure 3. The location of piezometers on the bed of the concave curvature of tunnel spillway in Alborz Dam

Table (1) indicates that piezometers located in the middle of the curvature have the largest pressures. This may be interpreted due to the flow has turned completely rotational at this location. The accord between the numerical and experimental results as depicted in Table (1) is satisfactory which leads to the conclusion that the RNG turbulent model is good for turbulent modeling in curvatures of tunnel spillways.

Table 1. Comparison of numerical and experimental pressure heads on the bed of the concave bend of the tunnel spillway of Alborz Dam

Piezometer No.	Inlet Discharge ($\mathbf{m^3}$/s)								
	950			800			600		
	Numerical(m)	Experimental (m)	Error%	Numerical (m)	Experimental (m)	Error%	Numerical(m)	Experimental (m)	Error%
1	20.00	23.76	18.78	3.79	2.04	25.50	7.70	5.40	19.40
2	25.98	30.64	17.93	19.66	14.24	27.59	14.6	11.24	23.00
3	29.40	33.34	13.36	22.80	26.42	15.87	16.0	19.77	23.56
4	32.44	34.41	6.07	25.79	30.76	19.27	18.6	22.19	18.75
5	32.60	33.50	2.76	25.92	28.79	11.05	18.7	22.79	21.40
6	30.92	30.59	1.08	24.84	26.95	15.87	18.3	22.45	22.13
7	18.22	21.07	15.64	14.41	18.40	15.87	10.8	22.19	20.32
MARE %			10.80			19.36			21.22

2.2. Dimensional analysis

The purpose of dimensional analysis is to convert the variables involved in the problem under consideration to dimensionless parameters. In this regard, the number of dimensionless parameters will be less than the involved variables which makes it easier to deal with the problem at hand. Since the flow in tunnel spillways is a free surface one with a high Reynolds Number, the inertia and gravity forces are the dominant forces in such flows. Thus, the Froude Number is considered as the dominant parameter in this problem, and the viscous forces which are represented by the Reynolds Number are neglected. Therefore, a relationship is sought for the selected variables in the problem under consideration in the form of

$$f(P_c.V.R.h.\rho.g) = 0 \tag{12}$$

Selecting $\rho, g,$ and $h,$ as repeating variables and using the Buckinham Pai theorem yields, $\frac{P_c}{\rho g h}, \frac{V^2}{gh}, \frac{h}{R}, \frac{h}{D}$ and θ as dimensionless parameters. The third dimensionless parameter can be divided by the fourth parameter to obtain $\frac{D}{R}$. Thus, the general dimensionless parameters will be $\frac{P_c}{\rho g h}, \frac{V^2}{gh}, \frac{D}{R}, \frac{h}{D}$ and θ. The goal is to develop a mathematical relationship among these dimensionless parameters in the form of the following function:

$$\frac{P_c}{\rho g h} = f\left(\frac{D}{R}.\frac{V^2}{gh}.\frac{h}{D}.\theta\right) \tag{13}$$

The pressure due to rotational flow acceleration, P_c in terms of the total pressure, $P,$ is

$$P_C = P - \rho g h \cos\theta \tag{14}$$

Substituting for P_C from Eq. (15) in Eq. (14) results in:

$$\frac{P - \rho g h \cos\theta}{\rho g h} = f\left(\frac{D}{R}.\frac{V^2}{gh}.\frac{h}{D}.\theta\right) \tag{15}$$

$\frac{V^2}{gh}$ is the Froude Number. This parameter is the most important in the problem because it represents the ratio of the inertial to the gravity forces in the problem.

f is an unknown function that has to be determined. A huge number of complicated functions can be selected to fit the above function which comprises four independent parameters. It is necessary to reduce the number of functions and obtain a relationship as simple as possible. In this regard, it is tried to take advantage of the physics of the problem at hand and the results obtained by other investigators. The main issue in this research is the pressure due to rotational flow acceleration which is in principle a function of the rotational acceleration, $\frac{V^2}{R.}$. It is noted that non of the dimensionless parameters in Eq. (15) include rotational acceleration. Multiplying the first and the second parameters results in $\frac{V^2}{gh}\frac{D}{R}$ which includes the rotational acceleration, $\frac{V^2}{R.}$. This means that it can be assumed that f should be a function of the multiplication of the first

and second parameters given in Eq. (15).

Referring to the real pressure distribution at the concave curvature of the tunnel spillway of Alborz dam and the results of Khani et al. [23] and the results of Flow-3D in this research, it is depicted that the pressure at the beginning of the curvature is low and equal to the hydrostatic pressure and increases along the curvature until it reaches a maximum around the middle of the curvature where the rotational flow is extremely established and starts then to decrease until the end of the bend at which the pressure is only hydrostatic. Thus, the dimensionless variable can be replaced by the dimensionless variable, $sin(2\theta)$ and multiplied by the parameter $\frac{V^2}{gh}\frac{D}{R}$ to produce $\frac{V^2}{gh}\frac{D}{R}\ sin(2\theta)$ which reflects the above-mentioned behavior of the pressure, i.e., equals to zero at the beginning and the end of the curvature. Thus, the function may be given as below:

$$\frac{P-\ \rho gh\cos\theta}{\rho gh} = f\left(\frac{V^2}{gh}\frac{D}{R}sin(2\theta), \frac{h}{D}\right) \tag{16}$$

It should be noted that $\frac{h}{D}$ is included in the parameter, $\frac{V^2}{gh}\ \frac{D}{R}sin(2\theta)$. Thus, it is probably an option not to consider it as a separate parameter. In this regard, the ANN was used to find a relation for $\frac{P-\ \rho gh\cos\theta}{\rho gh}$ in terms of the parameter $\frac{V^2}{gh}\frac{D}{R}sin(2\theta)$; i.e.:

$$\frac{P}{\rho gh} - \cos\theta = F\left(\frac{V^2}{gh}\ \frac{D}{R}\ sin(2\theta)\right) \tag{17}$$

2.3. Artificial neural network model

Artificial neural networks ANNs are classified based on the number of layers: single layer, multilayer, and based on the direction of information flow and processing feedforward. ANNs are massively parallel systems composed of many processing elements connected by links of variable weights. Of the many ANN paradigms, the multi-layer back propagation network (MLP) is by far the most popular (Lippman, [35]; Baylar et al., [36]).

The motivation for the development of neural network technology stemmed from the desire to develop an artificial system that could perform "intelligent" tasks similar to those performed by the human brain. The general structure of the neural network is depicted in Fig. (4) (Salmasi et al., [30]). It consists of input and output layers and many intermediate hidden layers between them. The number of hidden layers depends on the complexity of the problem at hand and it is determined by trial and error.

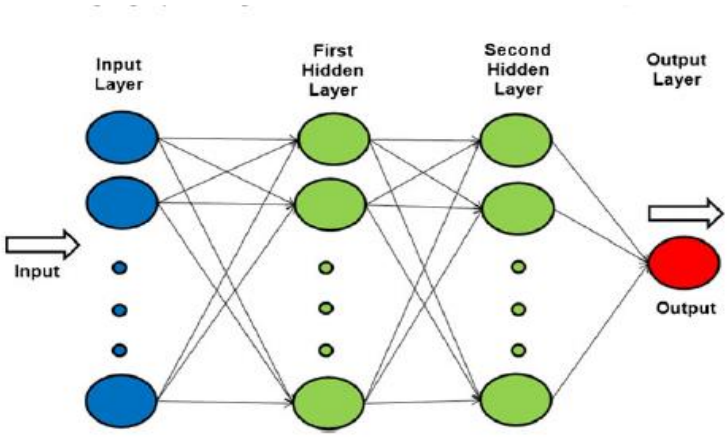

Figure 4. Structure of artificial neural network [37]

2.4. Development of an artificial neural network

In this study, a multi-layer feed-forward artificial neural network with a back propagation learning (FFBP) is used. The training function **TRAINLM,** the adaptation learning function **LEARNGDM** and the transfer function **TANSIG** are used in this research. The input data are selected as the variable $X = \left[\frac{V^2}{gh}\ \frac{D}{R}\ \sin(2\theta)\right]$ and the output/target data as $Y = \frac{P}{\rho gh} - \cos\theta$. These data should be normalized at the beginning to increase the speed of the neural network simulation. X and Y data have been normalized according to Eqs. (18) and (19) given below:

$$x_n = \frac{x_i - x_{min}}{x_{max} - x_{min}} \tag{18}$$

$$Y_n = \frac{Y_i - Y_{min}}{Y_{max} - Y_{min}} \tag{19}$$

Where X_{min} and X_{max} are minimum and maximum values of X's, respectively and Y_{min} and Y_{max} are minimum and maximum values of Y's, respectively.

The relation among the input data, hidden layers **neurons**, and the output data should be determined through the calibration process which is called the training stage. As mentioned earlier, the total number of the database consists of 659 X and Y pairs. 600 pairs are chosen in the training stage and 59 pairs are selected for the validation stage. Various numbers of hidden layers **neurons** are chosen in the training stage. 15 hidden layers **neurons** have given the highest correlation coefficient R^2 shown in Table (2).

Table 2. Results of ANN with various numbers of hidden layers

	artificial neural network		Simulated Neural Network and Flow-3D Results						
Model Number	Number of Data	Number of hidden layers neurons	Training	Validation	Testing	All	R^2	RMSE	MEA
1	600	3	0.9475	0.95255	0.93485	0.95037	0.9032	0.006191346	**0.018094385**
2	600	5	0.9639	0.93418	0.96046	0.95775	0.9173	0.005026743	**0.014688741**
3	600	7	0.95866	0.91758	0.95555	0.95881	0.9195	0.004417849	**0.012441036**
4	600	12	0.95788	0.9531	0.95181	0.9559	0.9137	0.004963657	**0.01435985**
5	600	15	0.96899	0.93406	0.92842	0.96801	0.9231	0.004390716	**0.012620211**
6	600	20	0.94128	0.93291	0.91278	0.93318	0.8708	0.003821044	**0.009629085**

3. Results of the artificial neural network

The result of the training stage in which 600 pairs are used is depicted in Fig. (5) and the result for the validation stage which is done for 59 pairs is shown in Fig. (6). Fig. (7) illustrates the proximity of the simulated results by the artificial neural network compared to the Flow-3D results which are used in this analysis as input data.

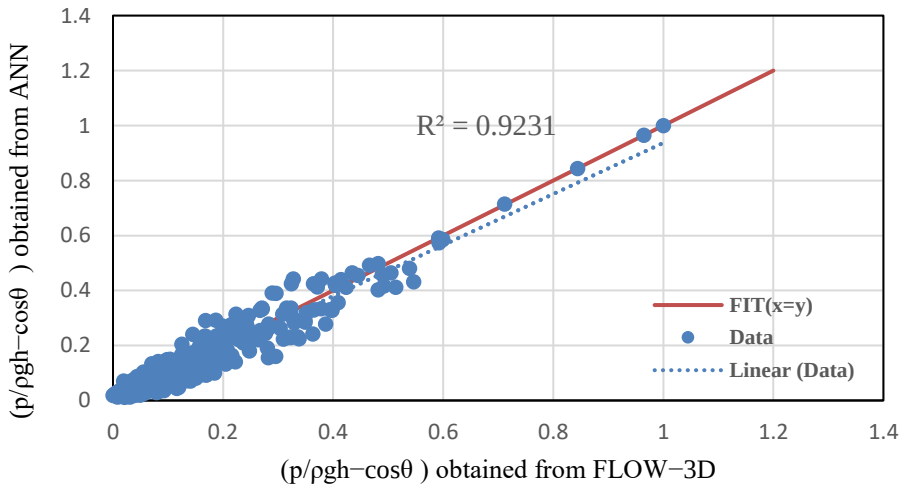

Figure 5. Correlation coefficient of the Neural Network simulation and Flow-3D in the training stage

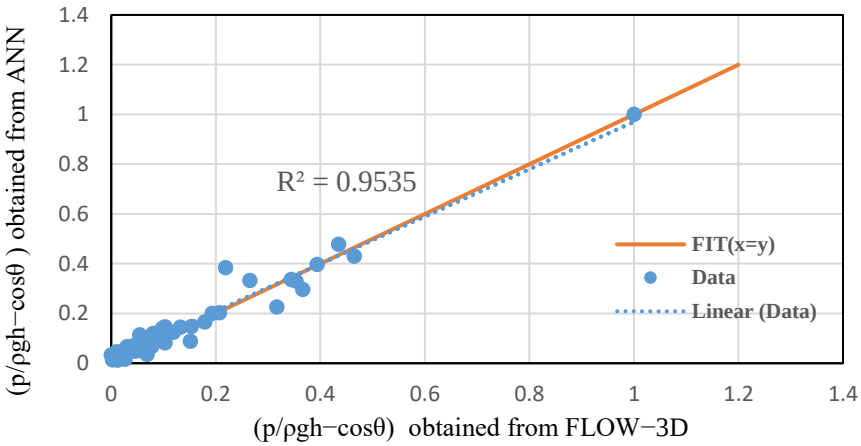

Figure 6. Correlation coefficient of the Neural Network simulation and Flow-3D in the validation stage

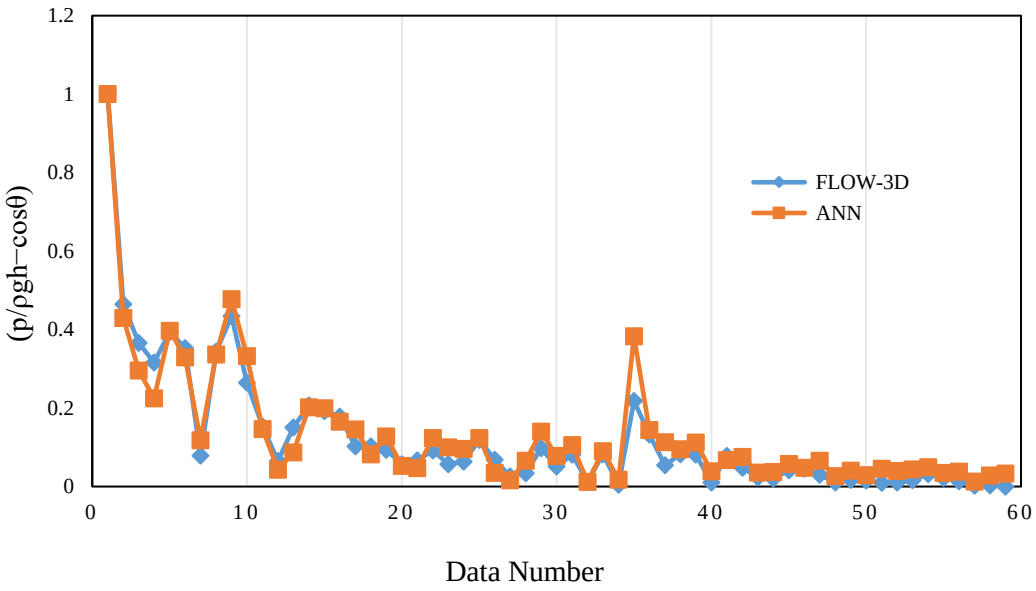

Figure 7. Comparison 0f the Simulated Neural Network and Flow-3D Results of the validation stage

3.1 Comparison of Neural Network Results with Common Relationships

Results obtained by the neural network and other common relationships given in Equations (1), (2), and (3) are shown in figs. (8–10). The results indicate that the neural network simulation gives much more accurate results compared to other common relationships.

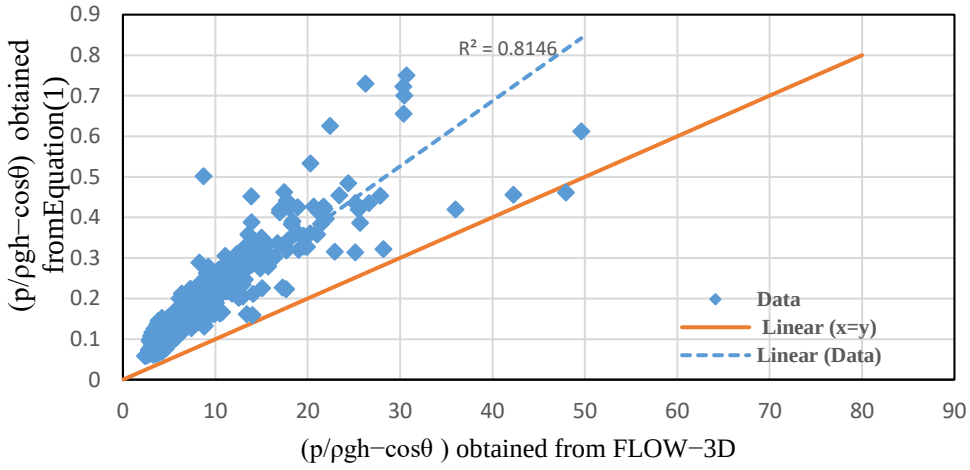

Figure 8. **Correlation coefficient of the Flow-3D numerical results and Equation (1)**

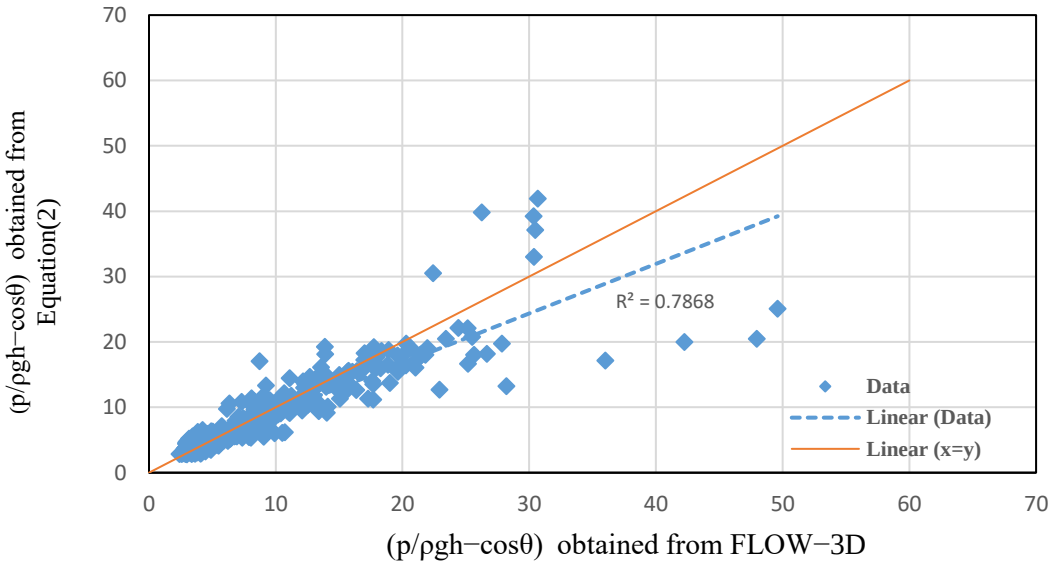

Figure 9. Correlation coefficient of the Flow-3D numerical results and Equation (2)

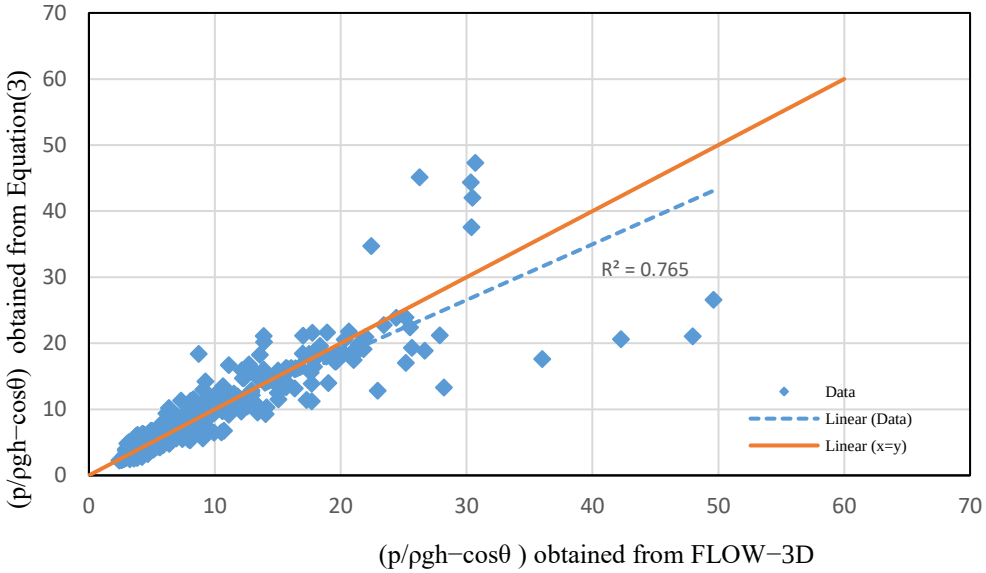

Figure 10. Correlation coefficient of the Flow-3D numerical results and Equation (3)

4. Summary and concluding remarks

In the present study, the FLOW-3D software was initially used to simulate the turbulent flow in tunnel spillways of various sizes and discharges. The results were verified by a comparison with the real data obtained from Alborz storage dam provided by the water research center of the ministry of energy in Iran.

Various turbulent models were used in the simulation and it was found that the RNG method results in the best agreement with the observed real results. Different tunnel spillways with diameters vary from 3 to 15 m, three different radii of curvature, and three discharges that cover almost all practical cases were used in the simulation. Dimensional analysis was utilized to produce dimensionless parameters and reduce the number of variables in the problem and finally, two main dimensionless groups were determined. The neural network is used to obtain a relation between these dimensionless variables and a correlation coefficient of 0.95 was obtained in the prediction stage of the pressure at concave bends of the tunnel spillways. The results of the pressure calculations were compared to those obtained by other common methods. The comparison indicates that the neural network results are much more accurate and it can be considered as a powerful tool to predict pressures at the concave curvatures of the spillway tunnels.

References

1. Kim, D. G., & Park, J. H. (2005). Analysis of flow structure over ogee-spillway in consideration of scale and roughness effects by using CFD model. KSCE Journal of Civil Engineering, 9(2), 161-169.

2. Sabbagh-Yazdi, S. R., Rostami, F., & Mastorakis, N. E. (2008, March). Simulation of self-aeration at steep chute spillway flow using VOF technique in a 3D finite volume software. In Am. Conf. on Appl. Maths. Harvard, Mass, 24-28.

3. Nohani, E. (2015). Numerical simulation of the flow pattern on morning glory spillways. International Journal of Life Sciences, 9(4): 28-31.
4. Parsaie, A., Dehdar-Behbahani, S., & Haghiabi, A. H. (2016). Numerical modeling of cavitation on spillway's flip bucket. Frontiers of Structural and Civil Engineering, 10(4), 438-444.
5. Teuber, K., Broecker, T., Bay´on, A., N¨utzmann, G. and Hinkelmann, R. (2019) 'CFD-modelling of free surface flows in closed conduits', Progress in Computational Fluid Dynamics, 19(6), 368–380.
6. Ghazanfari-Hashemi, R.S., Namin, M.M., Ghaeini-Hessaroeyeh, M. and Fadaei-Kermani, E., 2020. A Numerical Study on Three-Dimensionality and Turbulence in Supercritical Bend Flow. International Journal of Civil Engineering, 18(3), 381-391.
7. Sha, H. F., Wu, S. Q., & Zhou, H. (2009). Flow characteristics in a circular-section bend of high head spillway tunnel. Advances in Water Science, (6), 14.
8. Liu, Z., Zhang, D., Zhang, H., & Wu, Y. (2011). Hydraulic characteristics of converse curvature section and aerator in high-head and large discharge spillway tunnel. Science China Technological Sciences, 54(1), 33-39.
9. Zheng, Q. W., Luo, S. J., & Zhang, F. X. (2012). The Effect of Concave Types on the Hydraulic Characteristics in Spillway Tunnels with High-Speed Velocity. China Rural Water and Hydropower, 4.
10. Hongmin, G. U. O., Jiang, L. I., Shan, Q. I. N., & Yang, X. I. E. (2014). Three-Dimensional Numerical Simulation on Spillway Tunnel of Pankou Hydropower Station. Water Resources and Power, (4), 22.
11. Wan, W., Liu, B., & Raza, A. (2018). Numerical Prediction and Risk Analysis of Hydraulic Cavitation Damage in a High-Speed-Flow Spillway. Shock and Vibration, 2018.
12. Wei, W., Deng, J. and Xu, W. (2020). Numerical investigation of air demand by the free surface tunnel flows. Journal of Hydraulic Research, 1-8.
13. Xu, W., Dang, Y., Li, G., Shao, J. and Chen, G. (2007) 'Three-dimensional numerical simulation of the bi-tunnel spillway flow [J] ', Journal of Hydroelectric Engineering, 1, 56-60.
14. Huang, H.Y., Gong, A.M., Qiu, Y. and Wangliang, Z.A. (2015) ' 3D Numerical Simulation and Experimental Analysis of Spillway Tunnel' In Applied Mechanics and Materials. Trans Tech Publications Ltd. 723, 171-175.
15. Li, S., Zhang, J. M., Xu, W. L., Chen, J. G., Peng, Y., Li, J. N., & He, X. L. (2016). Simulation and experiments of aerated flow in curve-connective tunnel with high head and large discharge. International Journal of Civil Engineering, 14(1), 23-33.
16. Shilpakar, R., Hua, Z., Manandhar, B., Shrestha, N., Zafar, M. R., Iqbal, T., & Hussain, Z. (2017, August). Numerical simulation on tunnel spillway of Jingping-I hydropower project with four aerators. In IOP Conference Series: Earth and Environmental Science. 82, 012013.
17. Song, C. C., & Zhou, F. (1999). Simulation of free surface flow over spillway. Journal of Hydraulic Engineering, 125(9), 959-967.
18. Fais, L.M.C.F., Filho, J.G.D., Genovez, A.I.B. (2015). Geometry influence and discharge curve correction in morning glory spillways. Proceedings of the 36th IAHR World Congress.
19. Falvey, H. T. (1990). Cavitation in chutes and spillways. Denver: US Department of the Interior, Bureau of Reclamation. 49-57.
20. Chaudhry, M. H. (2007). Open-channel flow. Springer Science & Business Media.

21. Novak, P., Moffat, A. I. B., Nalluri, C., & Narayanan, R. (2007). Hydraulic structures. Fourth Edition, Taylor & Francis, New York , 246–265.
22. Jorabloo, M., Maghsoodi, R., Sarkardeh, H., & Branch, G. (2011). 3D simulation of flow over flip buckets at dams. Journal of American Science, 7(6), 931-936.
23. Khani, S., Moghadam, M. A., & Nikookar, M. (2017). Pressure Fluctuations Investigation on the Curve of Flip Buckets Using Analytical and Numerical Methods. Vol. 03(04), 165-171.
24. McCulloch, W. S., & Pitts, W. (1943). A logical calculus of the ideas immanent in nervous activity. The bulletin of mathematical biophysics, 5(4), 115-133.
25. Hopfield, J. J. (1982). Neural networks and physical systems with emergent collective computational abilities. Proceedings of the national academy of sciences, 79(8), 2554-2558.
26. Wu,C.L. Huang, B. Xie, C.B. (2008) . Comparison of calculation methods for irrigation district water inlet, China Rural Water and Hydropower ,5 (71) ,74–77.
27. Qiu,J. Huang, B.S. . Lai, G.W. (2002). Research and application of discharge coefficient of wide crest weir, China Rural Water and Hydropower ,9 ,41–42.
28. Xiang, H.Q .Ba,D.D. Liu, J.J. (2012) . Acquiring of curved practical weir flow coefficient by curve-fitting based on Matlab, Hydropower Energy Sci. 3 ,97–99.
29. Ye,Y.T. He,J.J.(2013).Experimental study on hydraulic calculation of discharge under plane gate on broad-crested weir, J. Water Resour. Archit. Eng. 11 (2), 138–141.
30. Salmasi, F., Yıldırım, G., Masoodi, A., & Parsamehr, P. (2013). Predicting discharge coefficient of compound broad-crested weir by using genetic programming (GP) and artificial neural network (ANN) techniques. Arabian Journal of Geosciences, 6(7), 2709-2717.
31. Noori, R.; Hooshyaripor, F. **(**2014). Effective prediction of scour downstream of ski-jump buckets using artificial neural networks. Water Resour. 41, 8–18.
32. Flow-Science. (2014). FLOW-3D user manual. version11. In: Flow Science Santa Fe, NM.
33. Yakhot, V. S. A. S. T. B. C. G., Orszag, S. A., Thangam, S., Gatski, T. B., & Speziale, C. G. (1992). Development of turbulence models for shear flows by a double expansion technique. Physics of Fluids A: Fluid Dynamics, 4(7), 1510-1520.
34. Report on the hydraulic model of Alborz dam reservoir. (2001). Iran Water Research Institute
35. Lippman, R. (1987). An introduction to computing with neural nets. IEEE Assp magazine, 4(2), pp.4-22.
36. Baylar, A., Ozgur, K.I.S.I. and Emiroglu, M.E. (2009). Modeling air entrainment rate and aeration efficiency of weirs using ANN approach. Gazi University Journal of Science, 22(2), 107-116.
37. Maureen, C. and Caudill, M. (1989). Neural network primer: Part I. AI Expert, 2(12), p.1987.